

# Hysteresis, Switching, and Negative Differential Resistance in Molecular Junctions: A Polaron Model

Michael Galperin,<sup>\*,†</sup> Mark A. Ratner,<sup>†</sup> and Abraham Nitzan<sup>‡</sup>

*Department of Chemistry and Nanotechnology Center, Northwestern University, Evanston, Illinois 60208, and School of Chemistry, The Sackler Faculty of Science, Tel Aviv University, Tel Aviv 69978, Israel*

Received October 28, 2004; Revised Manuscript Received November 13, 2004

## ABSTRACT

Within a simple mean-field model (self-consistent Hartree approximation) we discuss the possibility of polaron formation on a molecular wire as a mechanism for negative differential resistance (NDR), switching, and/or hysteresis in the  $I$ - $V$  characteristic of molecular junctions. This mechanism differs from earlier proposed mechanisms of charging and conformational change. The polaron model captures the essential physics and provides qualitative correspondence with experimental data. The importance of active redox centers in the molecule is indicated.

Substantial advances have recently been made in electron transport studies in molecular-scale systems.<sup>1–6</sup> An important goal here is molecular electronics to complement current Si technology. For example, negative differential resistance (NDR) was reported in several systems.<sup>7–12</sup> Bistability and hysteresis were reported in others.<sup>13,14</sup> These systems present an intrinsic challenge, to understand the structure/function relationships in such transport devices. Suggested possible mechanisms for NDR involve charging and/or conformational change.<sup>7,15,16</sup> No persuasive mechanism for such switching or hysteresis behavior is yet available.

Interestingly, these phenomena were observed mostly in molecular systems containing active redox centers, i.e., centers of long-living charged electronic states. This suggests the possibility of polaron formation on the molecule as a possible mechanism. Here we propose a simple polaronic model for NDR and hysteresis/switching behavior. Our analysis follows the mean field approximation of ref 17 and focuses on the steady-state behavior of such systems. After introducing the model, we study its properties showing the possibility for NDR and hysteresis behavior at equilibrium and under bias. Such modes of behavior appear already in the simplest possible one-site model for such redox systems.

Our molecular bridge is represented by one electronic level coupled to a single vibrational mode (“primary mode”) which in turn is coupled to a phonon bath that represents the thermal environment

$$\hat{H} = \epsilon_0 \hat{c}_0^\dagger \hat{c}_0 + \omega_0 \hat{a}^\dagger \hat{a} + \sum_{k \in \{L,R\}} \epsilon_k \hat{c}_k^\dagger \hat{c}_k + \sum_{k \in \{L,R\}} (V_k \hat{c}_k^\dagger \hat{c}_0 + h.c.) + M(\hat{a}^\dagger + \hat{a}) \hat{c}_0^\dagger \hat{c}_0 + \sum_{\beta} [\omega_{\beta} \hat{b}_{\beta}^\dagger \hat{b}_{\beta} + U_{\beta}(\hat{a}^\dagger + \hat{a})(\hat{b}_{\beta}^\dagger + \hat{b}_{\beta})] \quad (1)$$

where  $\epsilon_0$ ,  $\epsilon_k$  are energies of electronic states on the bridge and in the contacts, while  $\omega_0$ ,  $\omega_{\beta}$  are the primary and bath vibrational frequencies, respectively.  $V_k$  is the bridge-contacts coupling,  $M$  is electron–phonon interaction, and  $U_{\beta}$  is the coupling between the primary and bath phonons.  $\hat{c}_0$ ,  $\hat{c}_k$ ,  $\hat{a}$ , and  $\hat{b}_{\beta}$  and their adjoints are annihilation and creation operators for the electrons in the bridge level and in the contacts, and for the primary and bath phonons. We use units with  $\hbar = 1$ . The model can exhibit nonlinear transport behavior that stems from the fact that the energy of the resonant level shifts by polaron formation that in turn depends on the electronic occupation in that level. Here we investigate the nature and consequences of this nonlinearity using a mean-field (Hartree type) approximation.

Consider first the dynamics in the phonon subspace that, in the spirit of the Born–Oppenheimer (BO) approximation, sees the average electronic potential

$$\hat{H}_{\text{ph}} = \omega_0 \hat{a}^\dagger \hat{a} + M(\hat{a}^\dagger + \hat{a}) n_0 + \sum_{\beta} [\omega_{\beta} \hat{b}_{\beta}^\dagger \hat{b}_{\beta} + U_{\beta}(\hat{a}^\dagger + \hat{a})(\hat{b}_{\beta}^\dagger + \hat{b}_{\beta})] \quad (2)$$

where  $n_0 = \langle \hat{c}_0^\dagger \hat{c}_0 \rangle$  is the electronic population on the bridge

\* Corresponding author.  
† Northwestern University.  
‡ Tel Aviv University.

level. This Hamiltonian leads to a generalized quantum Langevin equation for the dynamics of the primary phonon

$$-\frac{1}{2\omega_0}\left(\frac{d^2}{dt^2} + \omega_0^2\right)(\hat{a} + \hat{a}^\dagger)(t) - \int_{-\infty}^{+\infty} dt' \Pi^r(t-t')(\hat{a} + \hat{a}^\dagger)(t') = Mn_0 + \hat{S}(t) \quad (3)$$

where the memory kernel

$$\Pi^r(t-t') = \sum_{\beta} U_{\beta} D_{0\beta}^r(t-t') U_{\beta} \quad (4)$$

is the retarded self-energy of the primary oscillator due to the phonon bath, and the noise operator is

$$\hat{S}(t) = \sum_{\beta} U_{\beta} (\hat{b}_{\beta} + \hat{b}_{\beta}^{\dagger})_0(t) \quad (5)$$

In eq 4,  $D_{0\beta}^r$  is the retarded Green function of the free phonon bath. The retarded Green function of the primary phonon  $D^r(t)$  is defined by

$$-\frac{1}{2\omega_0}\left(\frac{d^2}{dt^2} + \omega_0^2\right)D^r(t-t') - \int_{-\infty}^{+\infty} dt'' \Pi^r(t-t'')D^r(t''-t') = \delta(t-t') \quad (6)$$

In terms of this function the solution of eq 3 is

$$(\hat{a} + \hat{a}^\dagger)(t) = (\hat{a} + \hat{a}^\dagger)_0(t) + \int_{-\infty}^{+\infty} dt' D^r(t-t')Mn_0 + \int_{-\infty}^{+\infty} dt' D^r(t-t')\hat{S}(t') \quad (7)$$

The first term on the rhs is solution for primary phonon with damping, while next two terms come from interaction with the electron and bath phonons (source term). It follows that in steady-state

$$\langle(\hat{a} + \hat{a}^\dagger)\rangle = Mn_0 D^r(\omega=0) = -\frac{2\omega_0}{\omega_0^2 + (\gamma/2)^2} Mn_0 \quad (8)$$

where we have used in the wide-band approximation<sup>18</sup>

$$D^r(\omega) = \frac{1}{\omega - \omega_0 + i\gamma/2} - \frac{1}{\omega + \omega_0 + i\gamma/2} \quad (9)$$

Next consider the electron dynamics. Substituting eq 8 into eq 1 yields the effective electronic Hamiltonian

$$\hat{H}_{el} = \tilde{\epsilon}_0(n_0)\hat{c}_0^\dagger\hat{c}_0 + \sum_{k \in \{L,R\}} \epsilon_k \hat{c}_k^\dagger \hat{c}_k + \sum_{k \in \{L,R\}} (V_k \hat{c}_k^\dagger \hat{c}_0 + h.c.) \quad (10)$$

where

$$\tilde{\epsilon}_0(n_0) = \epsilon_0 - 2\epsilon_{\text{reorg}}n_0 \quad (11)$$

$$\epsilon_{\text{reorg}} = M^2 \frac{\omega_0}{\omega_0^2 + (\gamma/2)^2} \quad (12)$$

Note that level shift in eq 11 is proportional to  $2\epsilon_{\text{reorg}}$ . This corresponds to a static limit (BO approximation), when the oscillator is extremely slow, and an electron on the bridge interacts with constant static oscillator response corresponding to the average population on the bridge (for a detailed discussion see, e.g., ref 17).

Equation 10 is a simple single-level model, which can be treated in a standard way within the nonequilibrium Green function formalism.<sup>19</sup> For the steady-state situation and in the wide-band limit one gets for its occupation

$$n_0 = -i \int_{-\infty}^{+\infty} \frac{dE}{2\pi} G^<(E) = \int_{-\infty}^{+\infty} \frac{dE}{2\pi} \frac{f_L(E)\Gamma_L + f_R(E)\Gamma_R}{[E - \tilde{\epsilon}_0(n_0)]^2 + [\Gamma/2]^2} \quad (13)$$

where  $\Gamma = \Gamma_L + \Gamma_R$ ,

$$\Gamma_K = 2\pi \sum_{k \in K} |V_k|^2 \delta(E - \epsilon_k) \quad K = L, R \quad (14)$$

are electron escape rates to the contact  $K = L, R$ , assumed to be energy independent in the wide-band limit, and  $f_k(E) = [\exp\{(E - \mu_K)/k_B T\} + 1]^{-1}$  are the Fermi distribution functions with  $\mu_{L,R}$  being the electrochemical potentials in the contacts. Equation 13 is a self-consistent equation for  $n_0$ . In the  $T \rightarrow 0$  limit it takes the simpler form

$$n_0 = \frac{\Gamma_L}{\pi\Gamma} \arctan\left(\frac{\mu_L - \tilde{\epsilon}_0(n_0)}{\Gamma/2}\right) + \frac{\Gamma_R}{\pi\Gamma} \arctan\left(\frac{\mu_R - \tilde{\epsilon}_0(n_0)}{\Gamma/2}\right) + \frac{1}{2} \quad (15)$$

Consider first the zero temperature equilibrium situation  $\mu_L = \mu_R = \mu$  and  $T = 0$ . In this equilibrium case we can use eqs 15 and 11 to obtain two equations for  $n_0$  and an auxiliary variable  $x$

$$\begin{cases} n_0 = \frac{1}{\pi} \arctan(x) + \frac{1}{2} \\ n_0 = \frac{\Gamma}{4\epsilon_{\text{reorg}}}x + \frac{\epsilon_0 - \mu}{2\epsilon_{\text{reorg}}} \end{cases} \quad (16)$$

Equations 16 can have one or three solutions (see Figure 1), which implies possible bistability and hysteresis behavior. In this equilibrium case we can characterize the relative stability of the corresponding states by considering the free energy (or, at  $T = 0$ , the energy function) of a system restricted to population  $n_0$  on the bridge. The local density

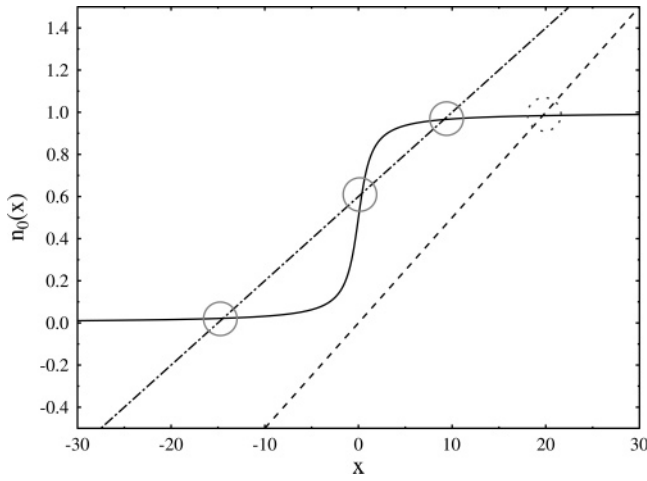


**Figure 1.** Functions  $n_0(x)$  of eq 16 plotted against  $x$ . Equation 16 can yield one (dotted circle) or three (solid circles) roots. Parameters are  $\Gamma = 0.2\epsilon_{\text{reorg}}$  and  $\epsilon_0 = \mu$  (dashed line);  $\Gamma = 0.16\epsilon_{\text{reorg}}$  and  $\epsilon_0 - \mu = 1.2\epsilon_{\text{reorg}}$  (dash-dotted line).

of states on the bridge is given by the spectral function, which in the wide band limit is

$$A(E, n_0) = \frac{\Gamma}{(E - \tilde{\epsilon}_0(n_0))^2 + (\Gamma/2)^2} \quad (17)$$

For a given  $n_0$ , define a local chemical potential  $\mu_0$  by

$$n_0 = \int_{-\infty}^{\mu_0} \frac{dE}{2\pi} A(E, n_0) \quad (18)$$

At unrestricted equilibrium and  $T = 0$   $\mu_0 = \mu$ , where  $\mu = (dE/dn)$  is the chemical potential on the leads. The roots  $n_r$  of eq 16 satisfy  $\mu_0(n_r) = \mu$ . To find the energy of a system restricted to a population  $n_0$  on the bridge we consider the total energy (level plus leads) change associated with transferring population  $dn$  from leads to bridge, which is given by  $dE_{\text{tot}} = (\mu_0(n) - \mu) dn$ . Upon integration from  $n_{\text{eq}}$  to  $n_0$  using eq 18 we get

$$E_{\text{tot}}(n_0) = E_{\text{tot}}(n_{\text{eq}}) + \frac{\Gamma}{2\pi} \log \left[ \frac{\cos \pi(n_{\text{eq}} - 1/2)}{\cos \pi(n_0 - 1/2)} \right] - \epsilon_{\text{reorg}}(n_0^2 - n_{\text{eq}}^2) + (\epsilon_0 - \mu)(n_0 - n_{\text{eq}}) \quad (19)$$

We choose  $n_{\text{eq}}$  to be the lowest energy root of eq 16 and set  $E_{\text{tot}}(n_{\text{eq}}) = 0$ . Stable equilibrium occupation  $n_0$  should provide a minimum of eq 19.

Figure 2a shows the function  $E_{\text{tot}}(n_0)$  obtained for the choice of parameters  $\mu = E_F = 0$  eV,  $\Gamma_L = \Gamma_R = 0.25$  eV,  $\omega_0 = 0.1$  eV,  $M = 0.3$  eV,  $\gamma_{\text{ph}} = 0.001$  eV (corresponding to  $\epsilon_{\text{reorg}} \sim 0.9$  eV). Extremum points correspond to the roots of eq 16 and indicate that the lowest and highest roots provide locally stable occupations, while the middle root represents an unstable occupation on the resonance level.

Figure 2b shows the hysteresis behavior of the stable level occupation  $n_r$  (lowest and highest roots) as a function of  $\epsilon_0$  (that can be changed in principle by a gate potential).

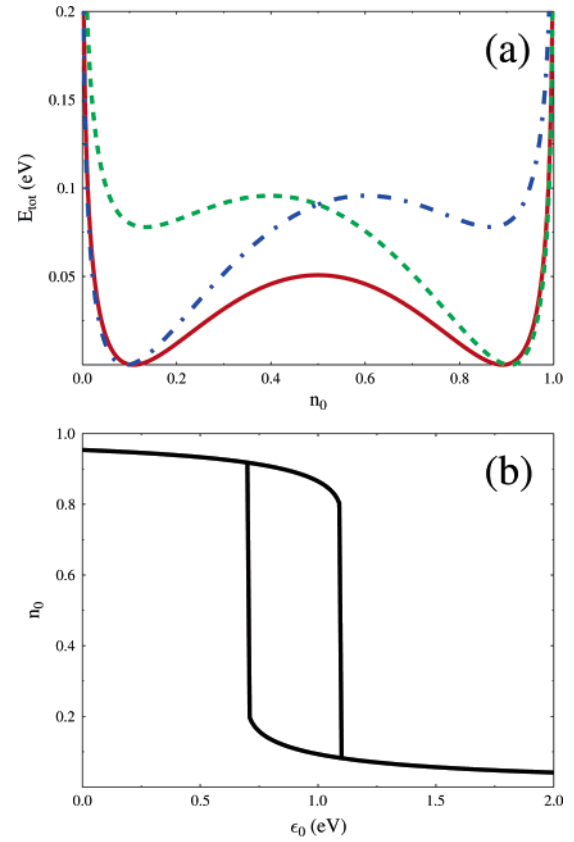


**Figure 2.** (a)  $E_{\text{tot}}$  (eq 19) plotted against  $n_0$  at  $T = 0$ . Three roots situations for  $\epsilon_0 = 0.8$  eV (dashed line),  $0.9$  eV (solid line), and  $1.0$  eV (dash-dotted line). (b) Stable roots  $n_r$  plotted against  $\epsilon_0$ . Parameters of this calculation are as in Figure 2a, but the calculation is done at  $T = 300$  K, i.e., eq 13 is used instead of eq 15.

Next consider the nonequilibrium case,  $\mu_L - \mu_R = V$ , and again start for simplicity with  $T = 0$ . The analogue of eq 16 now reads

$$\begin{cases} n_0 = \frac{\Gamma_L}{\pi\Gamma} \arctan\left(x + \frac{2\Gamma_R V}{\Gamma^2}\right) + \frac{\Gamma_R}{\pi\Gamma} \arctan\left(x - \frac{2\Gamma_L V}{\Gamma^2}\right) + \frac{1}{2} \\ n_0 = \frac{\Gamma}{4\epsilon_{\text{reorg}}} x + \frac{\epsilon_0 - E_F}{2\epsilon_{\text{reorg}}} \end{cases} \quad (20)$$

For definiteness we keep  $\epsilon_0$  fixed under imposed bias and take

$$\mu_L = E_F + \frac{\Gamma_R}{\Gamma} V \quad \mu_R = E_F - \frac{\Gamma_L}{\Gamma} V \quad (21)$$

This system can have one, three, or five solutions as shown in Figure 3.

In this nonequilibrium case we cannot define a function equivalent to  $E_{\text{tot}}(n_0)$ , whose extrema define stability. However, it seems reasonable that also here the outer roots are the physical (i.e., locally stable ones) and that in addition the middle root in the five-root case is locally stable.<sup>20</sup> This will obviously affect the hysteresis behavior. Indeed, in displays equivalent to Figure 2b we now find two hysteresis

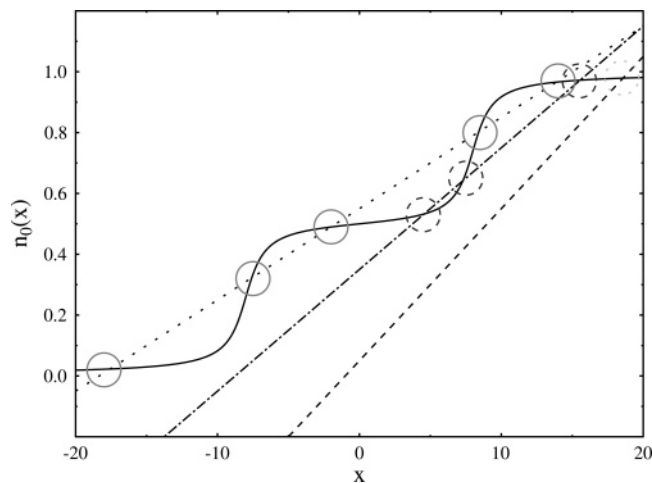


**Figure 3.** Graphs for functions  $n_0(x)$  as defined in eq 20. System can give one (dotted circle), three (dashed circles), or five (solid circles) roots. Parameters are  $\Gamma_L = \Gamma_R = 0.25$  eV,  $V = 4$  V, and  $\epsilon_{\text{reorg}} = 2.5$  eV and  $\epsilon_0 - E_F = 0.25$  eV (dashed line);  $\epsilon_{\text{reorg}} = 3.125$  eV and  $\epsilon_0 - E_F = 2.1875$  eV (dash-dotted line);  $\epsilon_{\text{reorg}} = 4.167$  eV and  $\epsilon_0 - E_F = 4.583$  eV (dotted line).

loops that may be traced to the resonance level crossing each chemical potential separately. In practice, gating such junctions is difficult; however, the signature of this hysteresis behavior can be seen in  $n_0/V$  plots (Figure 4a) that are relevant to the experimental results of ref 21 and in the predicted  $I-V$  characteristic of such junctions (Figure 4b). Focusing on the  $I-V$  behavior one can imagine a situation, where at  $V = 0$  the level is empty (situated above Fermi energy); upon increasing voltage bias (negative bias) one of the leads chemical potentials crosses the level position, thus partially filling it and consequently shifting its energy by polaron formation (or reorganization). A subsequent change in  $V$  in the opposite direction preserves the population up to some point, until recrossing takes place. This happens at different voltage at opposite bias compared with the negative sweep (due to the changed level position) and following that the level becomes empty again. This is qualitatively similar to the  $I-V$  characteristics presented in ref 13. Note, however, that the indicated route is not the only possible one. One could start with a filled rather than empty level. Also, when decreasing voltage from above 10 V in Figure 4 (or increasing from values below  $-10$  V), three possible routes (bifurcation points) exist. Our simple model cannot predict which of the routes will in fact be chosen. It is likely that in reality fluctuations or external factors (coupling to other molecules) will determine the hysteresis.

Finally we note that the polaron mechanism can also yield NDR features in the  $I-V$  characteristic. This can happen if the shift in the level energy upon occupation change moves it away from the window between the chemical potentials of the leads. Figure 5a shows an example using the parameters  $\epsilon_0 = 8.75$  eV,  $E_F = 0$  eV,  $\Gamma_L = \Gamma_R = 0.01$  eV,  $\omega_0 = 0.01$  eV,  $M = 0.224$  eV,  $\gamma_{\text{ph}} = 0.001$  eV, and  $T = 4$  K. The choice of  $M$ ,  $\omega_0$ , and  $\gamma_{\text{ph}}$  implies  $\epsilon_{\text{reorg}} \sim 5$  eV. The calculation is started from the filled level situation, and the observed NDR behavior is qualitatively similar to that of ref 7. Note that parameters chosen yield a position of the

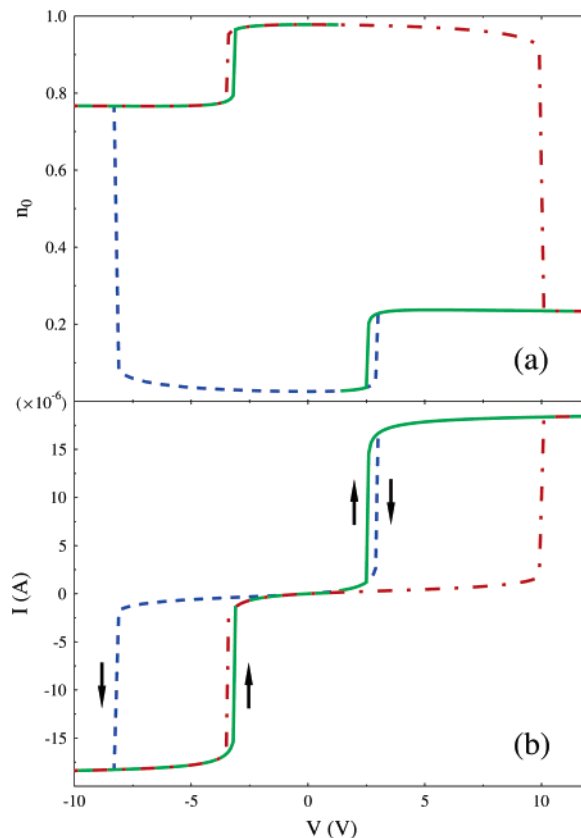


**Figure 4.** Nonequilibrium hysteresis behavior. Parameters are  $T = 300$  K,  $\Gamma_L = 0.1$  eV,  $\Gamma_R = 0.35$  eV,  $\omega_0 = 0.05$  eV,  $M = 0.4$  eV,  $\gamma_{\text{ph}} = 0.001$  eV, and  $\epsilon_0 = 3$  eV. Three curves on the graph represent situations of highest root (dash-dotted line), middle root (solid line), and lowest root (dashed line). (a) Hysteresis in occupation-voltage characteristic. (b) Hysteresis in current-voltage characteristic. One of the possible routes is marked by arrows.

filled level to be at  $\tilde{\epsilon}_0(n_0 = 1) = -1.25$  eV. The temperature dependence of the peak current and voltage show the right tendency (Figure 5b). The behavior described, however, depends on the bias sweep direction in contrast to experimental observation. Also note that the value used for the reorganization energy is unphysically large, implying that the model, as it stands, cannot be used for quantitative analysis of experimental results. Still, the model describes a generic property, and principles involved may prove relevant.

In conclusion, we have considered a simple resonant-tunneling junction with a bridge level coupled to a boson degree of freedom, in the Born-Oppenheimer approximation, which leads to a self-consistent Hartree approximation for the electron subspace of the problem. While the boson might represent solvent or electronic polarization, the consideration is most relevant for the case of extremely slow vibrations. The polaron coupling leads to a shift of the level position. This may yield hysteresis/switching and NDR features in the current/voltage characteristic, as shown in example calculations. Thus we suggest a polaronic mechanism as one more possibility (in addition to charging and conformational change of the molecule) for observing NDR and hysteresis/switching in molecular junctions. Conformational change implies alternation of the stereochemical geometry of the molecule, which is not relevant in our model.

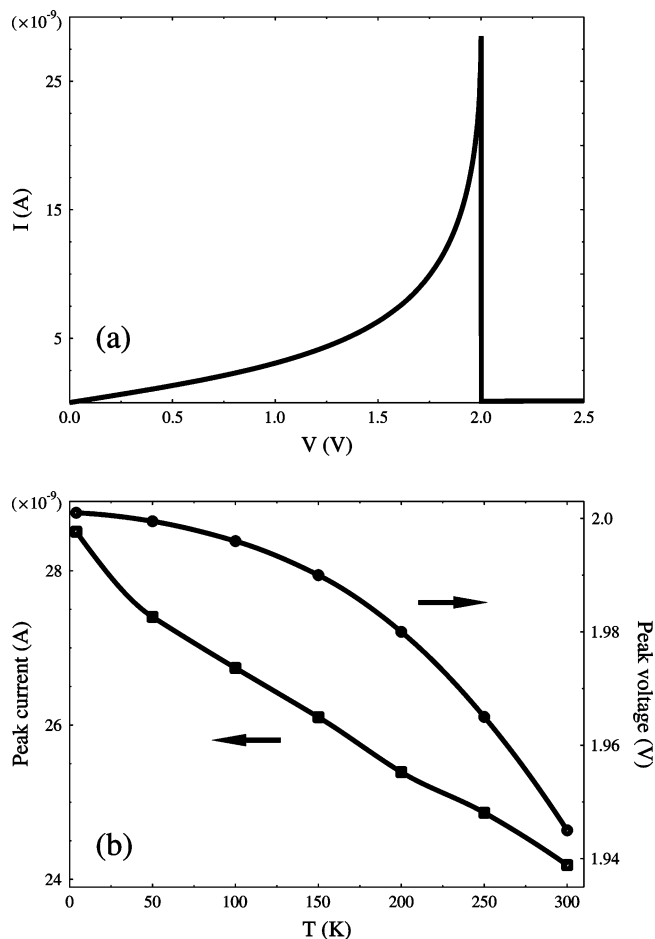


**Figure 5.** (a) NDR in current–voltage characteristic. Peak-to-valley ratio is 283:1. (b) Temperature dependence of the NDR peak current (left axis) and voltage (right axis).

On the other hand, the charging mechanism, while being similar to the polaron picture (the molecular site does change its charge), studied (de)localization of the presumable relevant molecular orbitals in static charged states of the molecule. As a result, previous approaches may be adequate to describe NDR, but not hysteresis. The polaron mechanism, by allowing dynamical change in  $n_0$  (the population of the molecule) provides a unified explanation for NDR and for hysteresis. The proposed mechanism conforms with the observation that only structures with active redox centers demonstrate NDR and hysteresis, as discussed in experimental papers.<sup>7–13</sup> This is because for polaron formation to occur, the electron has to spend enough time on the molecule. The current simple model captures the main physics, though more elaborate ones may be necessary to obtain quantitative correspondence with the experimental data.

Recent reports have examined multistable junctions from different perspectives;<sup>22</sup> here we have focused on the polaron mechanism as leading to hysteresis and NDR.

**Acknowledgment.** We are grateful to the DoD/MURI program, to the NSF-NCN program, and to the NASA–URETI program for support of this work. A.N. is grateful to Israel Science Foundation and the United States–Israel Binational Science Foundation.

## References

- (1) Joachim, C.; Gimzewski, J. K.; Aviram, A. *Nature* **2000**, *408*, 541.
- (2) Nitzan, A.; Ratner, M. A. *Science* **2003**, *300*, 1384. Nitzan, A. *Annu. Rev. Phys. Chem.* **2001**, *52*, 681. Davis, W. B.; Svec, W. A.; Ratner, M. A.; Wasielewski, M. R. *Nature* **1998**, *396*, 60.
- (3) Reichert, J.; Ochs, R.; Beckman, D.; Weber, H. B.; Mayor, M.; Löhneysen, H. *Phys. Rev. Lett.* **2002**, *88*, 176804. Reed, M. A.; Zhou, C.; Muller, C. J.; Burgin, T. P.; Tour, J. M. *Science* **1997**, *278*, 252. Weber, H. B.; Reichert, J.; Weigend, F.; Ochs, R.; Beckman, D.; Mayor, M.; Ahlrichs, R.; Löhneysen, H. *Chem. Phys.* **2002**, *281*, 113. Smith, R. H. M.; Noat, Y.; Untiedt, C.; Lang, N. D.; van Hemert, M. C.; Ruitenbeek, J. M. *Nature* **2002**, *419*, 906. Park, J.; Pasupathy, A. N.; Goldsmith, J. L.; Chang, C.; Yaish, Y.; Petta, J. R.; Rinkoski, M.; Sethna, J. P.; Abruna, H. D.; McEuen, P. L.; Ralph, D. C. *Nature* **2002**, *417*, 722. Liang, W. J.; Shores, M.; Bockrath, M.; Long, J. R.; Park, H. *Nature* **2002**, *417*, 725.
- (4) Kushmerick, J. G.; Pollack, S. K.; Yang, J. C.; Naciri, J.; Holt, D. B.; Ratner, M. A.; Shashidhar, R. *Ann. N. Y. Acad. Sci.* **2003**, *1006*, 277. Lee, T.; Wang, W. Y.; Klemic, J. F.; Zhang, J. J.; Su, J.; Reed, M. A. *J. Phys. Chem. B* **2004**, *108*, 8742.
- (5) Cui, X. D.; Primak, A.; Zarate, X.; Tomfohr, J.; Sankey, O. F.; Moore, A. L.; Moore, T. A.; Gust, D.; Harris, G.; Lindsay, S. M. *Science* **2001**, *294*, 571. Wold, D. J.; Frisbie, C. D. *J. Am. Chem. Soc.* **2001**, *123*, 5549.
- (6) Bumm, L. A.; Arnold, J. J.; Cygan, M. T.; Dunbar, T. D.; Burgin, T. P.; Jones, L.; Allara, D. L.; Tour, J. M.; Weiss, P. S. *Science* **1996**, *271*, 1705. Nazin, G. V.; Qui, X. H.; Ho, W. *Science* **2003**, *302*, 77. Datta, S.; Tian, W. D.; Hong, S. H.; Reifenberger, R.; Henderson, J. I.; Kubiak, C. P. *Phys. Rev. Lett.* **1997**, *79*, 2530.
- (7) Cai, L. T.; Skulason, H.; Kushmerick, J. G.; Pollack, S. K.; Naciri, J.; Shashidhar, R.; Allara, D. L.; Mallouk, T. E.; Mayer, T. S. *J. Phys. Chem. B* **2004**, *108*, 2827. Slowinski, K.; Chamberlain, R. V.; Miller, C. J.; Majda, M. *J. Am. Chem. Soc.* **1997**, *119*, 11910. Holmin, R. E.; Haag, R.; Chabinyk, M. L.; Ismagilov, R. F.; Cohen, A. E.; Terfort, A.; Rampi, M. A.; Whitesides, G. M. *J. Am. Chem. Soc.* **2001**, *123*, 5075.
- (8) Chen, J.; Reed, M. A.; Rawlett, A. M.; Tour, J. M. *Science* **1999**, *286*, 1550. Chen, J.; Wang, W.; Reed, M. A.; Rawlett, A. M.; Price, D. W.; Tour, J. M. *Appl. Phys. Lett.* **2000**, *77*, 1224.
- (9) Amlani, I.; Rawlett, A. N.; Nagahara, L. A.; Tsui, R. K. *Appl. Phys. Lett.* **2002**, *80*, 2761.
- (10) Kratochvilova, I.; Kocirik, M.; Zambova, A.; Mbindyo, J.; Mallouk, T. E.; Mayer, T. S. *J. Mater. Chem.* **2002**, *12*, 2927.
- (11) Walzer, K.; Marx, E.; Greenham, N. C.; Less, R. J.; Raithby, P. R.; Stokbro, K. *J. Am. Chem. Soc.* **1997**, *119*, S 2004, 126, 1229.
- (12) Rawlett, A. M.; Hopson, T. J.; Nagahara, L. A.; Tsui, R. K.; Ramachandran, G. K.; Lindsay, S. M. *Appl. Phys. Lett.* **2002**, *81*, 3043. Rawlett, A. M.; Hopson, T. J.; Amlani, I.; Zhang, R.; Tresek, J.; Nagahara, L. A.; Tsui, R. K.; Goronkin, H. *Nanotechnology* **2003**, *14*, 377.
- (13) Le, J. D.; He, Y.; Hoye, T. R.; Mead, C. C.; Kiehl, R. A. *Appl. Phys. Lett.* **2003**, *83*, 5518.
- (14) Li, C.; Zhang, D.; Liu, X.; Han, S.; Tang, T.; Zhou, C.; Fan, W.; Koehne, J.; Han, J.; Meyyappan, M.; Rawlett, A. M.; Price, D. W.; Tour, J. M. *Appl. Phys. Lett.* **2003**, *82*, 645. Schull, T. L.; Kushmerick, J. G.; Patterson, C. H.; George, C.; Moore, M. H.; Pollack, S. K.; Shashidhar, R. *J. Am. Chem. Soc.* **2003**, *125*, 3202.
- (15) Huber, J. L.; Chen, J.; McCormack, J. A.; Zhou, C. W.; Reed, M. A. *IEEE Trans.* **1997**, *44*, 2149. Chen, J.; Su, J.; Wang, W.; Reed, M. A. *Physica E* **2003**, *16*, 17.
- (16) Donhauser, Z. J.; Mantoath, B. A.; Kelly, K. F.; Bumm, L. A.; Monnell, J. D.; Stapleton, J. J.; Price, D. W., Jr.; Rawlett, A. M.; Allara, D. L.; Tour, J. M.; Weiss, P. S. *Science* **2001**, *292*, 2303. Seminario, J. M.; Zacarias, A. G.; Tour, J. M. *J. Am. Chem. Soc.* **2000**, *122*, 3015. Karzazi, Y.; Cornil, J.; Brédas, J. L. *Nanotechnology* **2003**, *14*, 165.
- (17) Karzazi, Y.; Cornil, J.; Brédas, J. L. *J. Am. Chem. Soc.* **2001**, *123*, 10076. Emberly, E. G.; Kirczenow, G. *Phys. Rev. B* **2001**, *64*, 125318.
- (18) Hewson, A. C.; Newns, D. M. *Proc. 2nd Int. Conf. Solid Surfaces, 1974; Japan J. Appl. Phys.* **1974**, *Suppl. 2*, Pt. 2, 121. Hewson, A. C.; Newns, D. M. *J. Phys. C: Solid State Phys.* **1979**, *12*, 1665.
- (19) Mahan, G. D. *Many-Particle Physics*; Kluwer Academic/Plenum Publishers: New York, 2000.
- (20) Haug, H.; Jauho, A.-P. *Quantum Kinetics in Transport and Optics of Semiconductors*; Springer-Verlag: Berlin, 1996.

(20) Indeed, in the Hartree approach, when we care only about total population of the resonant level, it is possible to introduce imaginary reservoir with one effective chemical potential, which will create the same level population as two reservoirs (contacts) out of equilibrium. With such substitution the true nonequilibrium picture is reduced to an effective equilibrium one. Then we can introduce energy of the system in exactly the same way it is done in the true equilibrium case.

(21) Repp, J.; Meyer, G.; Olsson, F. E.; Persson, M. *Science* **2004**, 305, 493.

(22) Gogolin, A.; Komnik, A. *cond-mat/0207513* **2002**. Alexandrov, A. S.; Bratkovsky, M. A.; Williams, R. S. *Phys. Rev. B* **2003**, 67, 075301. Mitra, A.; Aleiner, I.; Millis, A. J. *cond-mat/0409248* **2004**.

NL048216C